NOTE

Architecture-Driven Thermodynamic Interactions in Blends of Star-Branched and Linear Poly(methyl methacrylate)

T. D. MARTTER[1], M. D. FOSTER[1], K. OHNO[2], D. M. HADDLETON[2]

[1]The University of Akron, Maurice Morton Institute of Polymer Science, Akron, Ohio 44325

[2]The University of Warwick, Department of Chemistry, Coventry CV4 7AL, United Kingdom

Received 8 February 2002; revised 13 May 2002; accepted 13 May 2002

Keywords: star polymers; thermodynamics; neutron scattering

INTRODUCTION

In blends of two polymer chains of identical architecture, the bulk thermodynamic interaction can vary with differences in blend concentration, microstructure,[1] tacticity,[2] and isotopic labeling.[3,4] The strength of this interaction is typically expressed in terms of an effective segment–segment-interaction parameter, χ_{eff}, the value of which varies with all these molecular particulars. The fluctuation theory of Fredrickson et al.[5] suggests that if one component in a polymer blend is linear and the other has a long-chain branched architecture, the bulk interaction will increase over that in the case of an analogous blend with two linear components. This increase in the bulk interaction should manifest itself in an architectural contribution to the value of the χ_{eff} parameter derived from small-angle neutron scattering (SANS) data, although the architectural effect is intrinsically a nonlocal effect.

Recently, the magnitude of the architectural contribution to the bulk thermodynamic interaction has been probed experimentally in star/linear polystyrene (PS) blends and star/linear polybutadiene (PB) blends. Greenberg and coworkers[6–8] found that values of χ_{eff} for blends of star and linear PS measured with SANS increased monotonically with an increasing number of arms of the star, although the overall molecular weight of the stars was not kept rigorously constant and two different types of arm linking were used. Estimates of the thermodynamic interaction resulting from architectural effects alone, χ_ϵ, were made by measuring separately the magnitude of the interaction because of isotopic labeling and subtracting this from the value of the overall interaction, χ_{eff}. χ_ϵ increased with the number of arms of the star as expected from Fredrickson's theory,[5] but there was near-quantitative agreement only for the case of a four-arm star. The rate of change in the value of χ_ϵ with the number of star arms, p, was much larger for a change in p from 4 to 8 than when p increased from 14 to 21.

Martter et al.[9] measured the value of χ_{eff} for blends of star and linear PB with SANS and found that χ_{eff} and χ_ϵ varied nonmonotonically with an increase in the number of arms from 4 to 12. This result differed from the expectation from theory[5] that a monotonic increase in χ_ϵ with the number of arms of the star should be universally observed regardless of the chemical structure of the repeat unit. In this work, a brief study of star/linear blend for a third type of repeat unit was undertaken to further test the universality of the predictions of Fredrickson et al.[5] Poly(methyl methacrylate) (PMMA) was chosen because methods exist for the preparation of well-defined star polymers by atom transfer radical polymerization (ATRP). However, two other differences between the stars studied here and those examined previously must be noted. First, the star core chemistries differ from those used for the PS or PB stars as necessitated by the PMMA star synthesis. Although linear PMMA can be polymerized anion-

The Supplementary Material referred to in this article can be found at http://www.interscience.wiley.com/jpages/0887-6266/suppmat/0202017B.html

Correspondence to: M. D. Foster (E-mail: foster@polymer.uakron.edu)

Journal of Polymer Science: Part B: Polymer Physics, Vol. 40, 1704–1708 (2002)

Table 1. Molecular Characteristics of PMMA Polymers

Polymer	Name	M_n (g/mol) (SEC Linear Standards)	M_n (g/mol)[a]	N[b]	M_w/M_n[c]	N_{arm}
Linear PMMA	hPMMA	80,000	80,000	800	1.15	
4-Arm deuterated star	d4sPMMA	99,500	129,000	1200	1.11	300
7-Arm deuterated star	d7sPMMA	146,000	230,000	2100	1.26	300
14-Arm deuterated star	d14sPMMA	63,600	104,000	960	1.07	69
21-Arm deuterated star	d21sPMMA	60,000	112,000	1000	1.09	48

[a] From 5° LALS detected by SEC. M_n calculated as M_w(LALS)/(M_w/M_n).
[b] Assuming a segment molar volume of 100 cm^3/mol.
[c] Determined from a linear PMMA calibrated SEC.

ically, facile synthesis of PMMA stars of many arms using anionic techniques has not yet been achieved.[10] Second, the ATRP-polymerized polymers have arms terminated with bromine atoms, whereas the anionically polymerized PS and PB have arms terminated with *sec*-butyl initiator fragments. Limited study by the authors suggests that the distinctions in core chemistry[11] should be less important than the architecture effect, but the difference in chain-end functionality is more important in determining the overall effective interaction and the values of χ_ϵ extracted from the data.

EXPERIMENTAL

Deuterated star-branched PMMA (dPMMA) and linear PMMA (hPMMA) were synthesized by copper(I)-mediated living radical polymerization[12–15] at The University of Warwick. Functionalized pentaerythritol (see supplementary information) and cyclodextrin initiators[16–18] were used to initiate living radical polymerization of star polymers with target functionalities of 4 arms and 7, 14, and 21 arms, respectively. Size exclusion chromatography (SEC) analysis was carried out on a system equipped with a guard column and two 30-cm mixed D columns [Polymer Laboratories (PL)] with a differential refractive-index detector using tetrahydrofuran (THF) at 1 mL min^{-1} as an eluent. PMMA standards in the range of 200–1.64 $\times$ 10^6 g mol^{-1} were used to calibrate SEC. Absolute measurements of weight-average molecular weight (M_w) were made with a PL modular SEC equipped with a low-angle (5°) laser light scattering (LALS) detector and a concentration detector linked in series together with a guard column and two 30-cm mixed C columns (PL) using THF at 1 mL min^{-1} as an eluent. The refractive-index increment, dn/dc, was derived by integration of the concentration detector and used in the calculation of M_w. The light scattering cell of the SEC-LALS system was calibrated with narrow molecular weight PS standards (PL). ^{1}H and ^{13}C NMR spectra were recorded at 300 and 100 MHz on Bruker DPX300 and DPX400 spectrometers, respectively.

Molecular weights of the arms were determined by hydrolytic cleavage of the ester linkages connecting the arms of the stars under basic conditions with potassium hydroxide solution in a mixture of THF and methanol after the stars were synthesized. Some star–star coupling of polymers occurred during polymerization, and this coupling could be seen in the SEC curves. Removal of the coupled star polymers was accomplished by fractionation of the star product by precipitation. Molecular characteristics of the fractionated star polymers are listed in Table 1. Overall chain sizes are given in terms of the number of segments, N, for a segment molar volume of 100 cm^3/mol. Three of the star polymers formed a well-defined series in which the overall chain size was roughly constant while the number of arms varied. The overall molecular weight of the seven-arm star was markedly higher than the molecular weights of the other stars, but the arm molecular weights were the same for the four- and seven-arm stars, allowing for one comparison at constant arm size. SEC traces for all star polymers used in this study are given in the supplementary material.

The SANS samples were made by blending in a concentrated solution in benzene the appropriate amounts of the two components to yield a sample with a volume fraction of star of approximately 0.17. The linear component was the same for all blends. A majority of the solvent was evaporated at ambient conditions over approximately 1 day, before placing the samples under roughing vacuum at 70 °C for an additional 3 days. These samples were then pressed into 1.0-mm-thick brass rings at a temperature of 130 °C. SANS was measured over a range of scattering vector, q (= $4\pi\sin\theta/\lambda$), of 0.005–0.05 (1/Å) on the NG3 30-m SANS instrument at the Cold Neutron Research Facility at The National Institute of Standards and Technology with a sample-to-detector distance of 13 m, wavelength of 6 Å, relative wavelength resolution ($\Delta\lambda/\lambda$) of 0.150 full width at half-maximum, and one beam guide. To correct for incoherent scattering, a 100% hydrogeneous

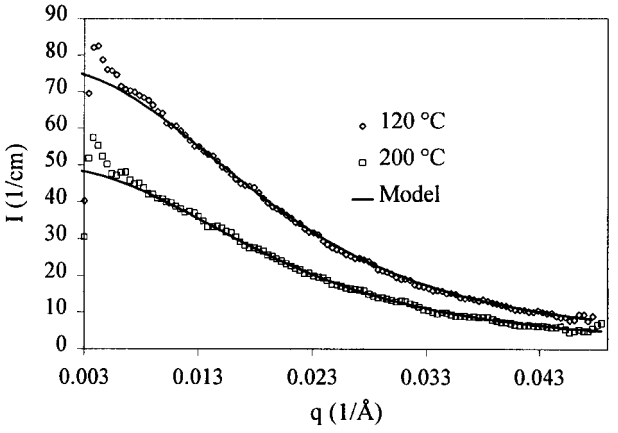

Figure 1. SANS experimental data with fits to RPA for a blend of 17% four-arm star dPMMA in a matrix of 83% linear hPMMA (d4shl) at 120 and 200 °C.

sample was also measured. The raw data were azimuthally averaged and then converted to absolute coherent scattering intensity as a function of q with the scattering measured from an isotopic PS blend standard sample.

RESULTS AND DISCUSSION

The scattering data for all SANS samples were fit with the Random Phase Approximation (RPA) approach[19–20] with the appropriate structure factors for the star[21,22] and linear polymers. More complete descriptions of fitting the SANS data for star/linear blends have been provided.[8,9] A previously measured value[23] of the segment length of 6.38 Å at 120 °C (for segment molar volume of 100 cm^3/mol) was used for both the star and linear PMMAs. Boothroyd et al.[23] have measured the change in segment length with temperature at 0.000319 Å/*K* in the temperature range of interest here. A published expression for the thermal-expansion coefficient[24] ($1.5 \times 10^{-6}T + 3.95 \times 10^{-5}$) was used to adjust the molar volume with changing temperature. This leaves χ_{eff} as the key parameter for fitting the scattering curves. A scaling factor of order unity that is intended to account for the presence of bubbles and systematic errors in the absolute intensity calibration was also required to obtain quantitative agreement over the whole range of q for each data set. Scattering curves and fits to RPA for a blend of a 17% four-arm star dPMMA with linear hPMMA (d4shl) are shown in Figure 1 for temperatures of 120 and 200 °C. Scattering for samples d4shl and d14shl was measured at temperatures of 120, 145, 170, and 200 °C, whereas for samples d7shl and d21shl scattering curves were measured only at temperatures of 120, 160, and 200 °C. Agreement between the experimental data and the model was good for the d4shl sample, whereas small discrepancies persisted at low values of q for samples d14shl and d21shl even for the "best fit" value of χ_{eff}. Sample d7shl had a distinctly different behavior because of the higher molecular weight of the seven-arm star. At 120 °C strong scattering at low values of q revealed that the blend was phase-separated. At 160 and 200 °C the scattering expression for a single phase blend represents the data reasonably well, but there are small discrepancies between the experimental data and the model not only at low values of q but also at intermediate values of q. We conjecture that this is due to the greater polydispersity of the seven-arm star.

For all the samples, the value of the scaling factor found from fitting the data dropped with increasing temperature. For the four- and seven-arm star blends, this factor was greater than 0.92 until it dropped to about 0.7 at 200 °C. For the 14- and 21-arm star blends, the values of the scaling factors were lower, and dropped correspondingly at higher temperature. We attribute the drop with temperature, at least in part, to the creation of bubbles in the sample because of the release of methyl bromide (MeBr) from thermal degradation of the chain end. Borman et al.[25] discovered with matrix-assisted laser desorption/ionization time-of-flight, evolved gas analysis, and ^{13}C NMR that when low molecular weight PMMA synthesized by ATRP and terminated with Br atoms was heated from room temperature to 150 °C, a loss of MeBr from the chain ends occurred that was followed by a cyclization reaction, giving a lactone chain end. Thermogravimetric analysis of the PMMA stars confirmed a weight loss of approximately 4% at 150 °C because of release of MeBr. We speculate that the low values of the scaling factor at low temperature found for the blends with the 14- and 21-arm stars may reflect increasing difficulties in modeling the stars with a Gaussian structure factor as the number of arms increases.

Temperature dependencies of χ_{eff} for the star/linear PMMA blends are exhibited in Figure 2. The key ob-

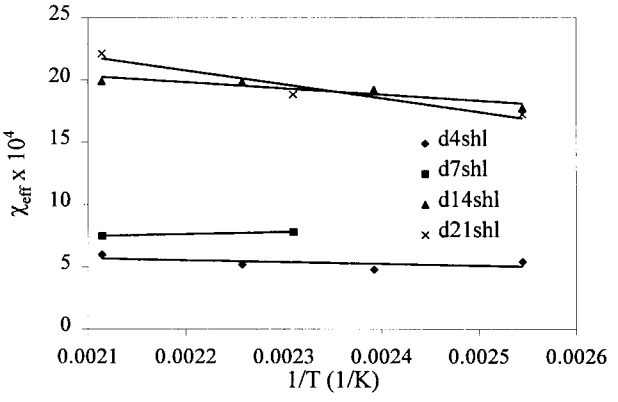

Figure 2. Interaction parameter as a function of inverse temperature for 17% 4-, 7-, 14-, and 21-arm star dPMMA mixed with linear hPMMA.

Table 2. Comparison of Theoretical and Experimental Values of χ_ε for Different Numbers of Arms of the Star

Number of Arms p	$\chi_\varepsilon \times 10^4$ (200°C) Experimental[a]	$\chi_\varepsilon \times 10^4$ (170°C) Experimental[a]	$\chi_\varepsilon \times 10^4$ (160°C) Experimental[a]	$\chi_\varepsilon \times 10^4$ (Universal Equation)[b] 200°C	$\chi_\varepsilon \times 10^4$ (Universal Equation)[b] 165°C
4	3.0	−.01	—	0.15	0.15
7	4.5	—	1.8	1.2	1.2
14	17	14.6	—	51	51
21	19	—	13	174	175

[a] Calculated by subtracting the value of χ_{eff} for a linear/linear blend from the value of χ_{eff} at the same temperature for the star/linear blend.
[b] Determined by eq 3.17 from ref. [5].

servation is that for the blends containing 4-, 7-, and 14-arm stars there are clear trends. First, χ_{eff} increased monotonically with an increasing number of arms of the star at the temperatures for which the blends were miscible, which agrees with the trend seen for the PS star/linear blends.[6−8] Both here and in the case of the PS blends this monotonic increase is seen despite the fact that the overall molecular weight is not kept constant. However, in the case of the PMMA blends, the variation in overall molecular weight is not large enough for the theory to anticipate the variation in molecular weight perturbing the order of the curves in Figure 2. The second trend is that the curves for the 4-, 7-, and 14-arm star blends are essentially parallel, indicating that the changes in χ_{eff} are entropic in nature. The third consistent trend for the three blends is that the temperature dependence of χ_{eff} is quite weak indicating that the isotopic effect itself is quite weak, weaker than that for PS blends and much weaker than that for PB blends. An important implication of this observation is that the phase separation seen in the case of the seven-arm star is largely driven by entropic considerations, not the isotopic effect. This observation seems to contradict the observations of Hopkinson et al.[4] who reported a much larger temperature dependence for isotopic linear/linear PMMA blends. A fourth observation is that the values of χ_{eff} are larger for the PMMA blends than for the PS blends containing stars with corresponding numbers of arms in the star (e.g., $\sim 5 \times 10^{-4}$ vs $\sim 1 \times 10^{-4}$ for the four-arm star), although the enthalpic contribution is weaker for PMMA.

Unfortunately it is difficult to assess the import of the data for the sample with the 21-arm star. However, it is included for completeness. For the two lower temperatures the value of χ_{eff} for the blend with the 21-arm star is the same as for the blend with the 14-arm star to within the experimental uncertainties. At 200 °C the value of χ_{eff} is higher for the 21-arm star blend than for the 14-arm star blend, but the 200 °C data are the least reliable. This difference for d21spmma could be due to its susceptibility to degradation by virtue of its high number of chain ends.

Quantitative comparison in Table 2 between the experimental values of χ_ϵ at 200 °C and theoretical values predicted from the theory of Frederickson et al.[5] reveals substantial discrepancies. Previously published results[4] for linear/linear PMMA blends were used to estimate the value of χ_{isotopic} for an isotopic linear/linear PMMA blend. For the blend with molecular weights closest to those we used, Hopkinson et al.[4] reported $\chi_{\text{isotopic}} = -0.0032 + 1.86/T$. The most important difference between the theoretical and experimental values is that the theory anticipates changes in the value of χ_ϵ of much greater magnitude (three orders) than are observed experimentally (~factor of 8). The experimental value of χ_ϵ for the four-arm star blend is much larger than the expectations of theory, whereas for the seven-arm star blend, the experimental value of χ_ϵ is only larger by a factor of 4. The value for the blend of the 14-arm star is less than the prediction by a factor of 3. The experimental value for the 21-arm star blend falls short of the prediction by around a factor of 10. Both experimentally derived values of χ_ϵ and theoretical predictions are shown for two temperatures. The theoretical predictions vary little with temperature because the temperature dependence of the segment length (and thus R_g) is small. The experimentally derived values differ with the temperature at which they are evaluated simply because the variation of χ_{eff} with temperature was different from that of the literature data for the isotopic linear/linear blend. This difference in slopes is unimportant to the comparison between experiment and theory for the blends with 14- and 21-arm stars, but for the comparisons for the 4- and 7-arm stars it has a significant impact on the apparent agreement between theory and experiment, revealing a substantial uncertainty in this comparison.

CONCLUSIONS

Measurement of the thermodynamic interaction as a result of star branching in a star/linear blend for a third type of polymer, PMMA synthesized by ATRP, indicated that the value of χ_ϵ increases monotonically

with the number of arms for numbers of arms up to 14. This is the same as seen for blends of anionically polymerized PS but different from blends of anionically polymerized PB. An apparent leveling off in the value of χ_ϵ as the number of arms increases to 21 is also consistent with the data from PS blends. To what degree core chemistry or chain-end chemistry effects contribute to differences in the absolute magnitude of the architectural effect between the PMMA blends and the PS and PB blends cannot be assessed with the existing materials.

The authors gratefully acknowledge financial support from the Army Research Office (contract DAAH04-96-1-0164). T. D. Martter thanks the LORD Corp. for a graduate fellowship. The authors acknowledge the support of the National Institute of Standards and Technology, U.S. Department of Commerce, in providing the neutron facilities supported through NSF-DMR-9423101. The authors also thank P. D. Butler for his help with the SANS measurements. The authors at The University of Warwick acknowledge funding from EPSRC (KO, GR/M74245) and the EPSRC network "Controlled Radical Polymerisation for Novel Functional Materials" (GR/N63765).

REFERENCES AND NOTES

1. Sakurai, S.; Jinnai, H.; Hasegawa, H.; Hashimoto, T.; Glen Hargis, I.; Aggarwal, S. L.; Han, C. C. Macromolecules 1990, 23, 451–459.
2. Beaucage, G.; Stein, R. S.; Hashimoto, T.; Hasegawa, H. Macromolecules 1991, 24, 3443–3448.
3. Graessley, W. W.; Krishnamoorti, R.; Balsara, N. P.; Fetters, L. J.; Lohse, D. J.; Schultz, D. N.; Sissano, J. A. Macromolecules 1993, 26, 1137–1143.
4. Hopkinson, I.; Kiff, F. T.; Richards, R. W.; King, S. M.; Munro, H. Polymer 1994, 35, 1722–1729.
5. Fredrickson, G. H.; Liu, A.; Bates, F. S. Macromolecules 1994, 27, 2503–2511.
6. Greenberg, C. C.; Foster, M. D.; Turner, C. M.; Corona-Galvan, S.; Cloutet, E.; Butler, P. D.; Hammouda, B.; Quirk, R. P. Polymer 1999, 40, 4713–4716.
7. Foster, M. D.; Greenberg, C. C.; Teale, D. M.; Turner, C. M.; Corona-Galvan, S.; Cloutet, E.; Butler, P. D.; Hammouda, B.; Quirk, R. P. Macromol Symp 2000, 149, 263–268.
8. Greenberg, C. C.; Foster, M. D.; Turner, C. M.; Corona-Galvan, S.; Cloutet, E.; Quirk, R. P.; Butler, P. D.; Hawker, C. J Polym Sci Part B: Polym Phys 2001, *39*, 2549–2561.
9. Martter, T. D.; Foster, M. D.; Yoo, T.; Xu, S.; Lizarraga, G.; Quirk, R. P.; Butler, P. D. Macromolecules, submitted for publication, 2002.
10. Quirk, R. P. University of Akron. Personal communication, January 2002.
11. Martter, T. D.; Foster, M. D.; Ohno, K.; Haddleton, D. M. Manuscript in preparation, 2002.
12. Haddleton, D. M.; Crossman, M. C.; Dana, B. H.; Duncalf, D. J.; Heming, A. M.; Kukulj, D.; Shooter, A. J. Macromolecules 1999, 32, 2110–2119.
13. Haddleton, D. M.; Jasieczek, C. B.; Hannon, M. J.; Shooter, A. J. Macromolecules 1997, 30, 2190–2193.
14. Haddleton, D. M.; Edmonds, R.; Heming, A. M.; Kelly, E. J.; Kukulj, D. New J Chem 1999, 23, 477–479.
15. Bon, S. A. F.; Steward, A. G.; Haddleton, D. M. J Polym Sci Part A: Polym Chem 2000, 38, 2678–2686.
16. Ohno, K.; Haddleton, D. M.; Kukulj, D.; Wong, B. Polym Prepr (Am Chem Soc Div Polym Chem) 2000, 41, 478–479.
17. Ohno, K.; Wong, B.; Haddleton, D. M. J Polym Sci Part A: Polym Chem 2001, 39, 2206–2214.
18. Wong, B.; Ohno, K.; Haddleton, D. Manuscript in preparation, 2002.
19. deGennes, P. G. Scaling Concepts in Polymer Physics; Cornell University Press: Ithaca, NY, 1979; pp 261–263.
20. Higgins, J.; Benoît, H. Polymers and Neutron Scattering; Oxford University Press: New York, 1994; p 225.
21. Benoît, H. C. J Polym Sci 1953, 11, 507.
22. Grest, G. S.; Fetters, L. J.; Huang, J. S.; Richter, D. Advances in Chemical Physics. In Polymeric Systems; Prigogine, I.; Rice, S. A., Eds.; Wiley: New York, 1996; Vol. 44, pp 67–163.
23. Boothroyd, A. T.; Rennie, A. R.; Wignall, G. D. J Chem Phys 1993, 99, 9135–9144.
24. Physical Properties of Polymers Handbook; Mark, J. E., Ed.; American Institute of Physics: Woodbury, NY, 1996; p 85.
25. Borman, C. D.; Jackson, A. T.; Bunn, A.; Cutter, A. L.; Irvine, D. J. Polymer 2000, 41, 6015–6020.